Cell Dynamics During Somite Boundary Formation Revealed by Time-Lapse Analysis

Paul M. Kulesa* and Scott E. Fraser†

We follow somite segmentation in living chick embryos and find that the shaping process is not a simple periodic slicing of tissue blocks but a much more carefully choreographed separation in which the somite pulls apart from the segmental plate. Cells move across the presumptive somite boundary and violate gene expression boundaries thought to correlate with the site of the somite boundary. Similarly, cells do not appear to be preassigned to a given somite as they leave the node. The results offer a detailed picture of somite shaping and provide a spatiotemporal framework for linking gene expression with cell movements.

Prevailing models of somite formation involve groups of cells within the presomitic mesoderm (the segmental plate) coalescing under the control of a slow-moving wavefront (in the anterior-to-posterior direction) and an intracellular oscillatory cycle within the cells (*1*–*8*). In such clock and wavefront models, the state of the cells in the cycle dictates what the cells should do when the wavefront triggers them. The result is repeated "slicing" of the presomitic mesoderm into somite-sized units. Other models suggest that neighboring cells are allocated to a particular somite during gastrulation coincident with or shortly after their exit from the node to join the presomitic mesoderm; these prespecified units later coalesce to form segments after counting a number of cell cycles or other oscillations (*9*–*17*). The recent explosion of molecular data (*18*–*23*) on genes that appear to march along with the segmentation pattern or localize near the forming somite after oscillating through the

Division of Biology, Beckman Institute 139-74, California Institute of Technology, Pasadena, CA 91125, USA.

*Present address: Stowers Institute for Medical Research, 1000 East 50th Street, Kansas City, MO 64110, USA.

†To whom correspondence should be addressed. E-mail: sefraser@caltech.edu

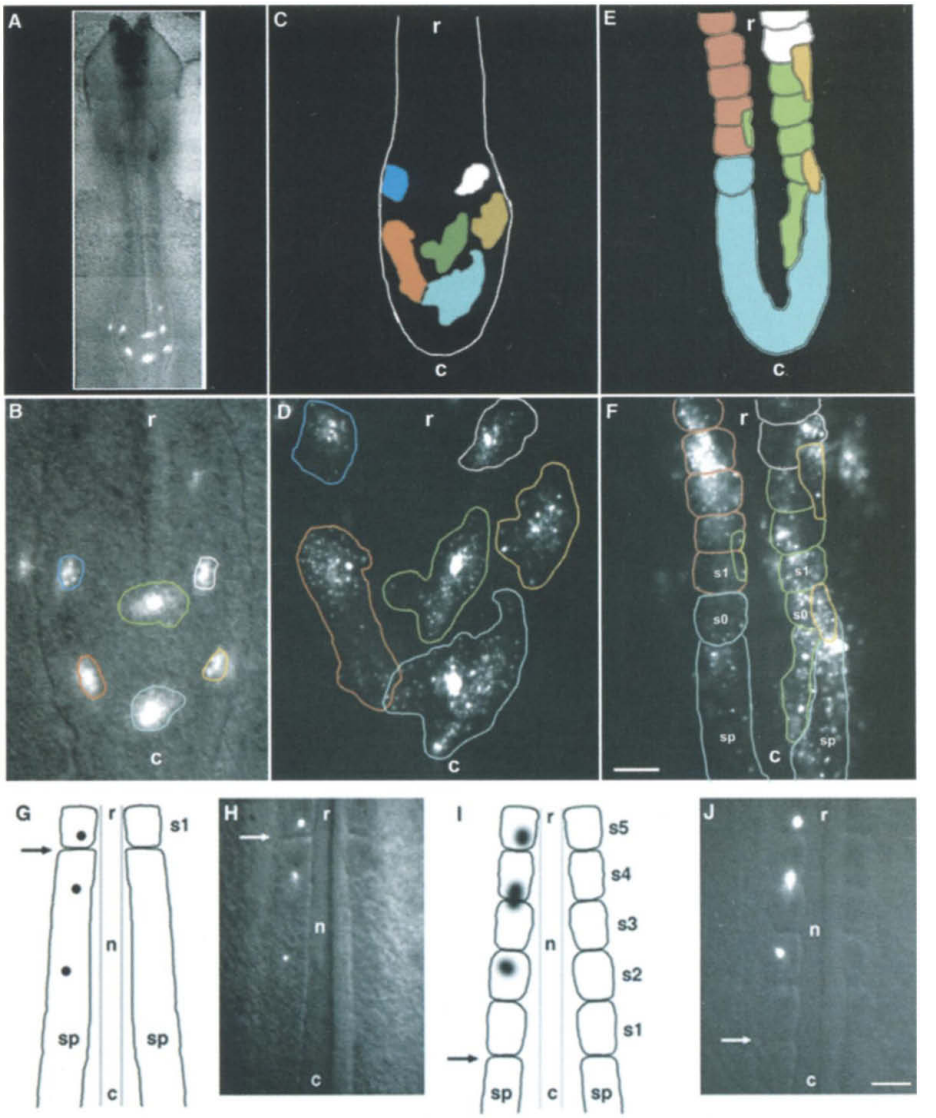

Fig. 1. Time-lapse series of DiI-labeled cells within the segmental plate. (**A** to **F**) Cells near the node frequently exchange neighbors and disperse. (A) Small numbers of cells are labeled at locations near the caudal end of the embryo. (B) Subgroups of the DiI-labeled cells in (A) are circled by different colors for clarity (r, rostral; c, caudal). [(C) and (D)] After 4 hours, cell dispersal and tissue movements spread the cells within the segmental plate shortly after release from the node. [(E) and (F)] After 16 hours, cells have spread extensively within the segmental plate (sp). (**G** to **J**) Within the range of segmentation, cells undergo minimal movements and maintain anteroposterior spacing. [(G) and (H)] Small numbers of cells are DiI-labeled at three different locations along the segmental plate on one side of the neural tube (n) in schematic (G) and raw data (H). The latest formed somite boundary is labeled (arrow). [(I) and (J)] Over 6 hours, the DiI-labeled cells disperse but remain within one somite length from the initial injection sites. Somite formation proceeds at the normal rate (~1.5 hours per somite pair) and occurs in the rostral-to-caudal direction. Scale bars in (F) and (J), 100 μm.

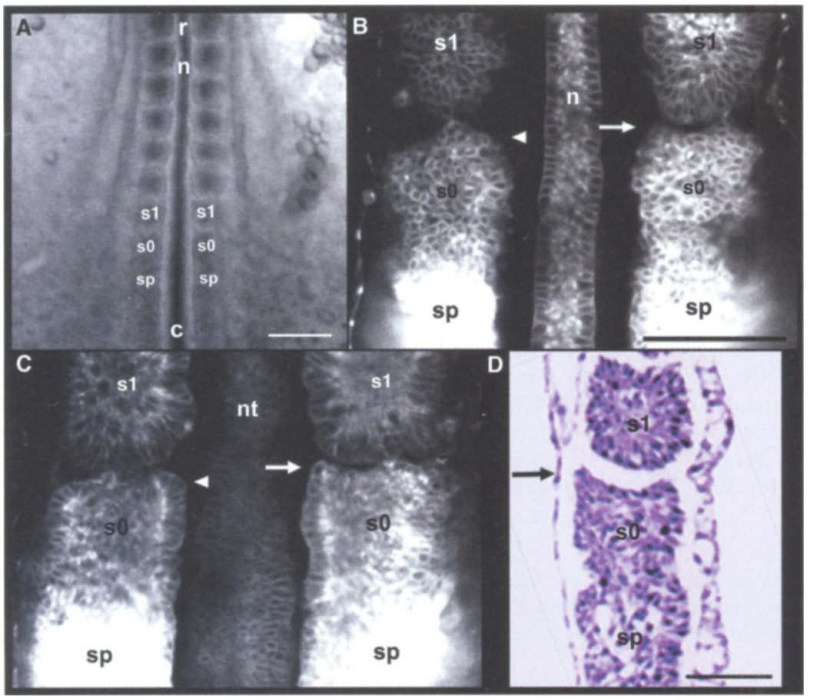

Fig. 2. Confocal images of fluorescently labeled live embryos and three-dimensional images of fixed tissue reveal a ball-and-socket shape to the separation of somite s0 from the segmental plate (sp). (**A**) Bright-field image of the embryo highlights the region of segmentation. (**B**) Typical confocal section shows the region near somite separation at the dorsoventral level of the notochord (n). (**C**) Deeper confocal sections into the tissue (>15 μm) reveal a ball-and-socket separation between the last formed somite (s1) and s0 (arrow) at the dorsoventral level of the neural tube (nt). (**D**) Surface imaging of a separate fixed embryo shows the ball-and-socket separation (arrow) within the tissue in sagittal section. The anterior borders of somite s0 are labeled (arrow and arrowhead) in (B) and (C). The rostral-to-caudal direction is labeled. Scale bars, 200 μm (A), 100 μm [(B) and (D)].

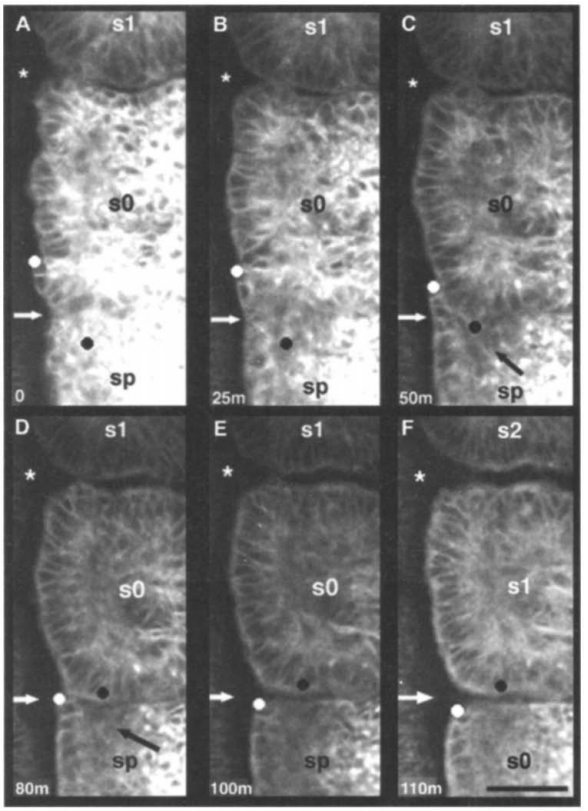

Fig. 3. Confocal time-lapse imaging series of fluorescently labeled tissue reveals that somite boundary formation occurs in a precise spatiotemporal order of six steps. (**A**) Initial sign of somite s0 separation from the segmental plate is marked by the separation of a sleeve of cells (white dot). At the same time, a second subgroup of cells in the segmental plate (black dot) coalesce. The presumptive somite boundary (white arrow) and anterior border of s0 (asterisk) are labeled. (**B**) The sleeve of cells (white dot) moves in the posterior direction, and the second subgroup of cells (black dot) begins to move in the anterior direction. (**C**) The anterior movement of the second subgroup of cells (black dot) leaves a gap in the tissue in the anterior portion of the segmental plate (black arrow). (**D**) The sleeve of cells (white dot) folds into the gap in the segmental plate while the second subgroup of cells (black dot) becomes integrated into s0. (**E**) The sleeve of cells (white dot) becomes part of the anterior border of the segmental plate, and the cells from the segmental plate (black dot) form part of the posterior border of s0. (**F**) Completion of the posterior border transforms s0 into s1. Scale bar, 50 μm; elapsed time is in minutes.

length of the presomitic mesoderm over one somite cycle has reawakened interest in this fascinating process. There is now a critical need for spatial information about the local cell movements and shape changes during somite formation and a means to accurately register gene expression patterns with the local morphological changes in the tissue.

In answer to this challenge, we have designed techniques to visualize individual cell movements, cell morphology, and tissue shaping within the segmental plate during somite formation in living whole chick embryo explants. The embryos are maintained intact in a chamber with a coverslip bottom and covered above by an oxygen-permeable membrane (*24*). To visualize cell movements within the segmental plate, we followed small groups of cells labeled with 1,1′-dioctadecyl-3,3,3′,3′-tetramethylindocarbocyanine perchlorate (DiI) from the time when cells enter the segmental plate near the posterior node region, move along the segmental plate, and then contribute to somites. We find that in the node region, cells actively exchange neighbors and disperse, spreading cells throughout large regions of the segmental plate (Fig. 1, A to F) (movie S1). Within a range of four or five somites from the anterior end of the segmental plate, cells disperse less, executing only short-range motions of less than a somite length (Fig. 1, G to J) (movie S2).

Three-dimensional imaging of fluorescently labeled cells within living embryos through the segmental plate reveals differences in the tissue morphology near the site where the somite separates from the segmental plate (Fig. 2). We define the most recently formed somite (with complete anterior and posterior borders) as s1 (Fig. 2, A and B). The anterior portion of the segmental plate is the site of the forming somite, termed s0, and prospective somites are denoted consecutively in the posterior direction as s-1, s-2, and so on. At the dorsoventral level of the notochord, the separation of the next somite from the segmental plate appears as a gap on the medial and lateral sides of the segmental plate (Fig. 2B) (movie S3). Deeper into the tissue, the boundary is not straight; instead, a ball (forming somite) and socket (segmental plate) separation of tissue becomes apparent (Fig. 2C). Serial sections of fixed tissue in sagittal views confirm the ball-and-socket separation shape throughout the center of the somite tissue (Fig. 2D).

Steps in somite formation. How does somite s0 become s1? Time-lapse confocal microscopy of bodipy-ceramide–labeled embryos reveals a series of well-ordered steps that appear to be choreographed to create a somite boundary (see movies S4 and S5). In the first step, a small number of cells in the rostral-medial region of the segmental plate (Fig. 3A, white dot), adjacent to the neural tube and rostral to the presumptive somite boundary (white arrow), coalesce into a distinct subgroup and separate slightly from the

segmental plate tissue (Fig. 3B). This subgroup of cells appears as a sleeve about one cell thick and extending about five cell diameters rostral of the presumptive boundary between s0 and the segmental plate (white arrow). At about the same time, a second subgroup of cells within the segmental plate organizes into a cluster (Fig. 3, A and B; near black dot), extending about four cell diameters posterior to the presumptive border between s0 and the segmental plate (white arrow). We identify this step as tissue separation.

In the next step, there is an exchange of these two subgroups of cells across the presumptive somite boundary. The first subgroup of cells (within s0) (Fig. 3B, white dot) begins to move as a unit in the posterior direction (Fig. 3, B to D; white dot). At the same time, the second subgroup of cells (in the segmental plate) (Fig. 3B, black dot) moves collectively in the anterior direction (Fig. 3, B to D; black dot). The two subgroups of cells slide past each other in opposing directions, creating a gap on the medial side of the segmental plate (Fig. 3, B to D).

The next step completes the somite boundary between s0 and the segmental plate, thus conferring s1 status to somite s0. In this step, the two subgroups of cells integrate into different sides of the somite boundary. The sleeve of cells on the medial side, adjacent to the neural tube, folds in toward the forming somitic cleft (Fig. 3, D to F; white dot) framing the anterior corner of s0 (Fig. 3F, white dot). The second subgroup of cells (which originated from the segmental plate) is absorbed into somite s1 to form part of the posterior border of s1 (Fig. 3F, black dot). In time-lapse sequences, the two movements appear to be choreographed, as the sleeve falls into the gap left by the subgroup of cells that moves anteriorly from the segmental plate (movies S4 and S5). As the two subgroups of cells slide past one another, the separation of tissue between the somite and the segmental plate propagates in the medial-to-lateral direction to separate somite s0 and the segmental plate (Fig. 3, C to F; white arrow) and so s0 becomes s1 (separated by a distinct cleft from the segmental plate). The caudal border of this new s0 is formed by the same sequence of three steps described above.

The sculpting of the entire somite s0 involves an epithelialization process that takes place gradually over the time period of one somite cycle starting at the anterior border of s0 and continuing in the posterior direction, finishing at the posterior border of somite s0 as it separates from the segmental plate (see movies S4 and S5). The first signs of epithelialization of s0 take place at its anterior border and along the medial side of s0 (Fig. 3, A and B). This process continues along the medial side in the anterior half of s0 (Fig. 3, A and B). In contrast, cells closer to the center and within the posterior half of the forming somite remain fairly rounded (Fig. 3, A and B), as does the sleeve of cells (Fig. 3, white dot). As s0 begins to separate from the segmental plate and form its posterior border, cells within the posterior half of s0 gradually rearrange to become more densely packed and columnar (Fig. 3, C to F). When s0 separates from the segmental plate, its structure has an epithelial appearance, resembling a closely packed circumferential ring of columnar-shaped cells, elongated in the radial direction (Fig. 3, E and F).

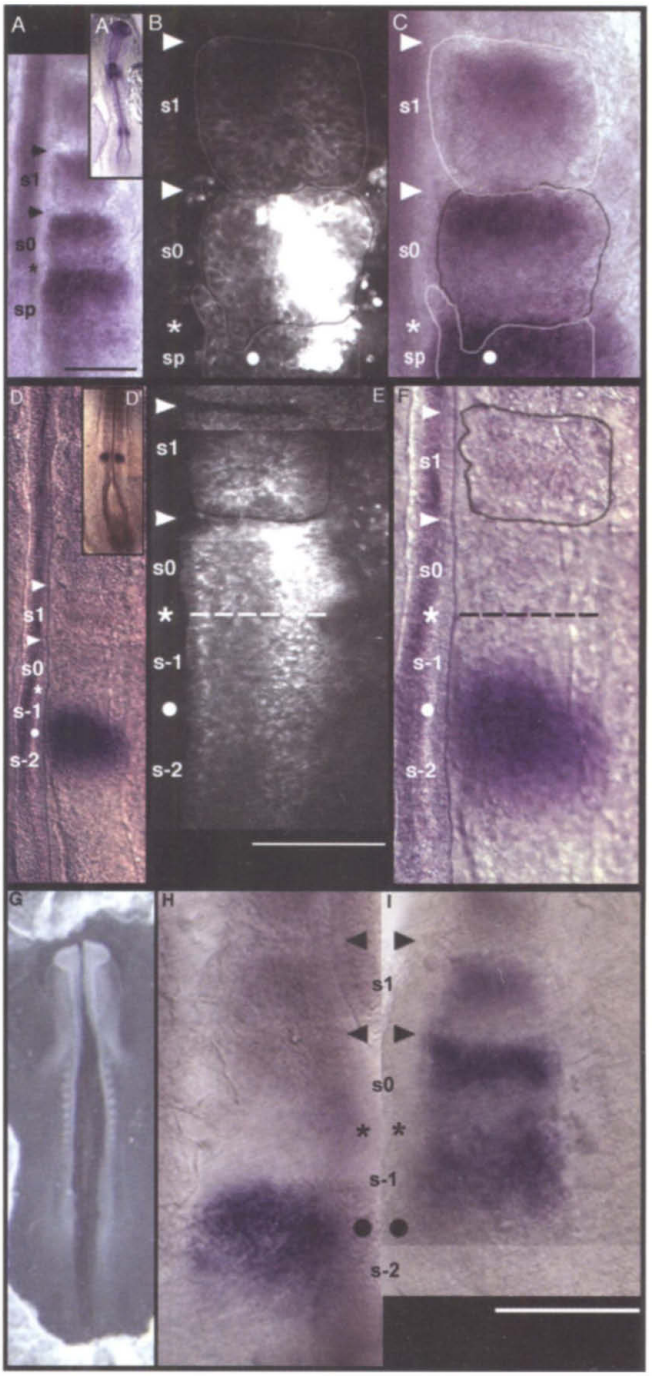

Fig. 4. Comparison of two key gene expression patterns (*EphA4* and *cMeso-1*) with cell positions in the same embryo (**A** to **F**) and on either side of the neural tube within the same embryo (**G** to **I**). (A) Typical *EphA4* expression pattern within the somites and the embryo (A′). The anterior and posterior borders of somite s1 (arrowheads) and the presumptive somite boundary between s0 and the segmental plate (asterisk) are labeled. (B) Confocal section of fluorescently labeled tissue near s0 shows the outlines drawn around the subpopulations of cells that will become part of each somite. (C) Same embryo as in (B) shows the expression pattern of *EphA4*, with the somite outlines. The sleeve of cells does not express *EphA4* (just anterior to the asterisk). However, the subgroup of cells within the segmental plate (white dot) does express *EphA4*. These two subgroups of cells will soon move across the presumptive somite boundary and change gene expression to maintain the characteristic pattern of *EphA4*. (D) Typical pattern of expression of *cMeso-1* within the somites and the embryo (D′). Anterior and posterior borders of somite s1 (arrowheads), approximate position of the forming somite boundary (asterisk), and future somite boundary between s-1 and s-2 (s-1/s-2) (white dot) are labeled. (E) Confocal section of fluorescently labeled tissue in the region of s0 shows that s0 has not begun to separate from the segmental plate (dashed line). (F) In the same embryo as in (E), *cMeso-1* expression straddles s-1/s-2 (white dot) and covers a region of about one somite in anteroposterior length. There is no expression of *cMeso-1* at the site where s0 will soon separate from the segmental plate (asterisk and dashed line). [(G) to (I)] Side-by-side comparison of *EphA4* and *cMeso-1* in the same embryo shows there is very little overlap between the expression patterns. (G) A typical embryo is cut in half along the anteroposterior axis, fixed, and in situ hybridized with the particular gene probes. (H) *cMeso-1* expression appears to straddle the future s-1/s-2 boundary (black dot). [(G) and (I)] There is very little overlap between the expression of *EphA4* and *cMeso-1* (black dot) near s-1/s-2, and *cMeso-1* does not appear to be expressed in the area where s0 will break off from the segmental plate (asterisk). Scale bars, 200 μm (A), 100 μm [(E) and (I)]; each somite is about 100 μm across in (B) and (C).

Although the structure of the somite is formed, there are still very dynamic movements of cells within the somite. In time-lapse movies, cells actively divide within the epithelial ring and move back and forth in radial directions, sometimes exchanging with the mesenchymal core of cells in the center (see movies S4 and S5).

Boundaries and gene expression domains. To investigate the relationship between segmental gene expression and future somite boundaries, we compared cell positions with gene expression boundaries in the same animal for two different genes (*24*). We first compared cell positions and the expression boundaries of *EphA4* (*25*). *EphA4* is expressed in the anterior portion of the segmental plate, in an anteroposterior graded expression within s0 and within the anterior half of s1 (Fig. 4A). From time-lapse imaging sequences, cell positions before and during somite boundary formation are identified immediately before the fixation of each individual embryo. In the first example, we identify the two subgroups of cells that will be exchanged across the presumptive somite boundary: the receding sleeve of cells from somite s0 (Fig. 4B, asterisk) and cells from the segmental plate, which will move in the anterior direction into somite s0 (Fig. 4B, white dot). The sleeve of receding cells (the first subgroup described above) does not express *EphA4* (Fig. 4C, asterisk); however, these cells will move to and become part of the anterior border of the forming somite and a region of strong *EphA4* expression. Cells within the segmental plate (the second subgroup) express *EphA4* (Fig. 4, B and C; white dot) and within a matter of minutes will move in the anterior direction into the posterior part of somite s0, a region with a low level of *EphA4* expression (Fig. 4C).

We also compared the forming somite boundaries with the expression of *cMeso-1* (*26*), a gene thought to play a role in demarcating future somite boundary sites. The expression of *cMeso-1* covers an anteroposterior range of about one somite (Fig. 4D); however, we find that *cMeso-1* is not expressed in the area where s0 will break off from the segmental plate (Fig. 4F; asterisk, dashed line). Instead, *cMeso-1* expression straddles the prospective s-1/s-2 somite boundary (Fig. 4F, white dot) at a time when the anterior border of somite s0 has just folded inward (Fig. 4E, arrowhead) and s0 has not begun to separate from the segmental plate (Fig. 4E, asterisk). Thus, *cMeso-1* expression appears to mark the sites of prospective somite boundaries—the s-1/s-2 or s-2/s-3 boundaries, not the forming somite boundary.

To validate the preceding results, we determined the spatial relationships between the expression patterns of *EphA4* and *cMeso-1*. We used each half of the embryo in the same animal (cut along the midline of the neural tube; Fig. 4G) to simultaneously compare two gene expression patterns (*24*). Because *EphA4* is expressed in the area where s0 separates from the segmental plate, we used its expression pattern as the reference mark (Fig. 4I). Our results show that there is very little overlap between the expression of *EphA4* and that of *cMeso-1* (Fig. 4, H and I). *cMeso-1* expression appears about one somite length away from the next somite boundary (Fig. 4, H and I; asterisk), having anterior borders of expression closer to a prospective somite boundary (Fig. 4, H and I; black dot).

Dynamic processes shape somites. Our results show that a somite boundary is not simply related to gene expression patterns. We chose *EphA4* as an example of a gene whose expression appeared to correlate with the segmentation pattern and has a repeating periodicity. The *Eph* family has been implicated in the formation of rhombomere boundaries in the hindbrain, another segmented system in vertebrates, and it seems likely that *Eph* family members play a role in somite segmentation (*23, 27–29*). Our comparison of *EphA4* expression, the presumptive boundary of s0, and the segmental plate shows that the straight-line expression of *EphA4* does not match the ball-and-socket–shaped separation of the tissue to form the somite boundary. Instead of driving the cell separation at the somite boundary, it appears that gene expression lags behind the motions. The cells that move across the presumptive somite boundary must rapidly change expression of *EphA4* to match the expression pattern becoming restricted to the anterior half of s1.

Our DiI labeling results show that cells do not simply march out and maintain order along the segmental plate so that a simple boundary forms between previously fated anterior and posterior neighbors. Labeled cells frequently exchange neighbors and widely disperse, so that the order in which cells exit the node is not predictive of their later fate. Further anterior along the segmental plate, cells appear to approximately maintain anteroposterior spacing, suggesting that cells begin to settle into an approximate cluster when within range of segmentation.

Our findings show that the sculpting of somites in chicks is a more involved process than was previously thought, violating current models of somite segmentation. Somitogenesis occurs in a precise spatiotemporal order of six steps involving tissue separation, cell movements, and integration of cells at the anterior and posterior somite borders (Fig. 5). Somite separation is not a simple, straightforward slicing. Three-dimensional imaging of bodipy-ceramide–labeled live embryos and fixed tissue shows that a somite pulls apart from the segmental plate. Time-lapse analyses reveal that this ball-and-socket tissue separation is followed by a series of complex movements in which cells move across the presumptive somite boundary and violate gene expression boundaries thought to correlate with the site of the somite boundary. The results fill a major void in our previous knowledge base of the temporal dynamics of somite formation and motivate a model for somite formation in which both dynamic gene expression and cell motions pattern and sculpt the presomitic mesoderm into somites.

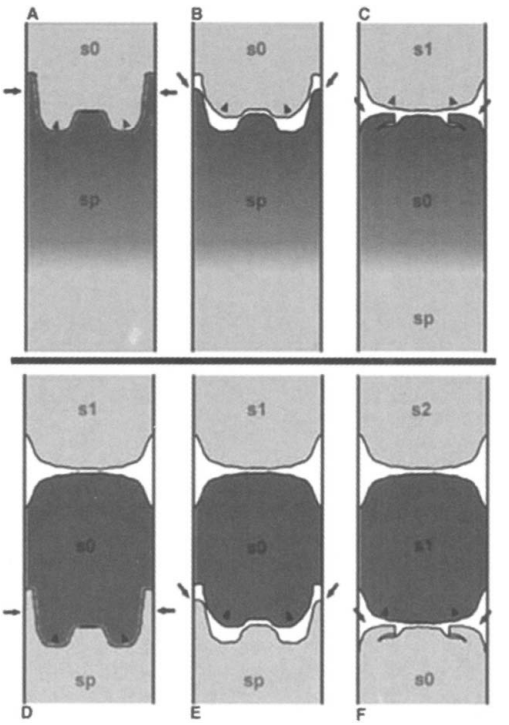

Fig. 5. Sculpting of a somite takes place in a series of six repeatable steps shown in schematic form. (**A**) Anterior border of a somite forms when tissue from the neighboring, more anterior somite (s0) separates from the medial and lateral sides of the segmental plate (arrows). A second subgroup of cells (arrowheads) coalesces in the segmental plate. (**B**) The first subgroup of cells (arrows) slides in the posterior direction while the second subgroup of cells moves in the anterior direction (arrowheads). (**C**) The first subgroup of cells folds in toward the somite center into gaps in the tissue left from segmental plate cells, which have moved in the anterior direction. These cells form the anterior border of s0. The second subgroup of cells becomes absorbed into the posterior border of s1 (arrowheads). (**D** to **F**) At the posterior end of somite s0, the same process takes place to separate somite s0 from the segmental plate.

References and Notes

1. J. Cooke, E. C. Zeeman, *J. Theor. Biol.* **58**, 455 (1976).
2. H. Meinhardt, in *Somites in Developing Embryos*, R. Bellairs, D. A. Ede, J. W. Lash, Eds. (Plenum, New York, 1986), pp. 179–189.
3. J. Cooke, *Trends Genet.* **14**, 85 (1998).
4. I. D. Barrantes *et al.*, *Curr. Biol.* **9**, 470 (1999).
5. A. Aulehla, R. L. Johnson, *Dev. Biol.* **207**, 49 (1999).
6. Y. J. Jiang *et al.*, *Nature* **408**, 475 (2000).
7. K. J. Dale, O. Pourquie, *Bioessays* **22**, 72 (2000).
8. J. Dubrulle, M. J. McGrew, O. Pourquie, *Cell* **106**, 219 (2001).
9. R. Bellairs, *Bull. Zool.* **47**, 245 (1980).
10. A. G. Jacobson, S. Meier, in *Somites in Developing Embryos*, R. Bellairs, D. A. Ede, J. W. Lash, Eds. (Plenum, New York, 1986), pp. 1–16.
11. P. P. L. Tam, P. A. Trainor, *Anat. Embryol.* **189**, 275 (1994).
12. A. Wood, P. Thorogood, *Dev. Dyn.* **201**, 151 (1994).
13. C. D. Stern, S. E. Fraser, R. J. Keynes, D. R. N. Primmett, *Development* **104** (suppl.), 231 (1988).
14. D. R. N. Primmett, W. E. Norris, G. J. Carlson, R. J. Keynes, C. D. Stern. *Development* **105**, 119 (1989).
15. J. Collier *et al.*, *J. Theor. Biol.* **207**, 305 (2000).
16. S. Schnell, P. K. Maini, *Dev. Dyn.* **217**, 415 (2000).
17. M. Kerszberg, L. Wolpert, *J. Theor. Biol.* **205**, 505 (2000).
18. F. E. Stockdale, W. Nikovits, B. Christ, *Dev. Dyn.* **219**, 304 (2000).
19. R. Keller, *Curr. Top. Dev. Biol.* **47**, 183 (2000).
20. H. L. Stickney, M. J. F. Barresi, S. H. Devoto, *Dev. Dyn.* **219**, 287 (2000).
21. C. A. Henry, L. A. Hall, M. Burr-Hille, L. Solnica-Krezel, M. S. Cooper. *Curr. Biol.* **10**, 1063 (2000).
22. O. Pourquie, *Annu. Rev. Cell Dev. Biol.* **17**, 311 (2001).
23. Y. Saga, H. Takeda, *Nature Rev. Genet.* **2**, 835 (2001).
24. See supporting data on *Science* Online.
25. C. Schmidt, B. Christ, M. Maden, B. Brand-Saberi, K. Patel, *Dev. Dyn.* **220**, 377 (2001).
26. A. Buchberger, K. Seidl, C. Klein, H. Eberhardt, H. H. Arnold, *Dev. Biol.* **199**, 201 (1998).
27. K. Sakamoto *et al.*, *Biochem. Biophys. Res. Commun.* **234**, 754 (1997).
28. Q. Xu, G. Mellitzer, V. Robinson, D. G. Wilkinson, *Nature* **399**, 267 (1999).
29. L. Durbin *et al.*, *Genes Dev.* **12**, 3096 (1998).
30. A. J. Ewald, H. McBride, M. Reddington, S. E. Fraser, R. Kerschmann, *Dev. Dyn.*, published online 11 October 2002 (10.1002/dvdy.10169).

31. We thank M. Dickinson and J. Kastner for comments on the manuscript and help with in situ hybridizations, and A. Ewald, H. McBride, M. Reddington, and R. Kerschman for their help with the serial sectioning by surface imaging microscopy (*30*). P.M.K. is a participant in the California Institute of Technology Initiative in Computational Molecular Biology, which is funded by a Burroughs Wellcome Fund Interfaces award.

Supporting Online Material

www.sciencemag.org/cgi/content/full/298/5595/991/DC1
Materials and Methods
Movies S1 to S5

27 June 2002; accepted 28 August 2002

Contribution of Human α-Defensin 1, 2, and 3 to the Anti–HIV-1 Activity of CD8 Antiviral Factor

Linqi Zhang,[1]* Wenjie Yu,[1] Tian He,[1] Jian Yu,[1] Rebecca E. Caffrey,[2] Enrique A. Dalmasso,[2] Siyu Fu,[2] Thang Pham,[2] Jianfeng Mei,[2] Jaclyn J. Ho,[1] Wenyong Zhang,[1] Peter Lopez,[1] David D. Ho[1]*

It has been known since 1986 that CD8 T lymphocytes from certain HIV-1–infected individuals who are immunologically stable secrete a soluble factor, termed CAF, that suppresses HIV-1 replication. However, the identity of CAF remained elusive despite an extensive search. By means of a protein-chip technology, we identified a cluster of proteins that were secreted when CD8 T cells from long-term nonprogressors with HIV-1 infection were stimulated. These proteins were identified as α-defensin 1, 2, and 3 on the basis of specific antibody recognition and amino acid sequencing. CAF activity was eliminated or neutralized by an antibody specific for human α-defensins. Synthetic and purified preparations of α-defensins also inhibited the replication of HIV-1 isolates in vitro. Taken together, our results indicate that α-defensin 1, 2, and 3 collectively account for much of the anti–HIV-1 activity of CAF that is not attributable to β-chemokines.

T lymphocytes that carry the CD8 antigen play a critical role in controlling HIV-1 or simian immunodeficiency virus (SIV) replication in vivo (*1*). The initial control of viremia after primary infection is temporally correlated with the onset of virus-specific CD8 cytotoxic T lymphocytes (CTLs) (*2*, *3*). SIV replication in macaques increases dramatically when a monoclonal antibody (mAb) is used to deplete CD8 T cells (*4*, *5*). Moreover, the strong pressure exerted by cellular immunity in vivo is apparent from the rapid emergence of CTL-escape viruses (*6*, *7*). Although the direct killing of infected cells by CD8 CTLs is important in virus suppression (*1*), soluble factors secreted by CD8 T lymphocytes can also inhibit HIV-1 or SIV replication in vitro. In 1986, Walker *et al.* (*8*) first described the CD8 antiviral factor (CAF), a diffusible molecule secreted by stimulated CD8 T cells from certain HIV-1–infected individuals. Unlike the activity of CTLs, the antiviral activity of CAF is noncytolytic and does not require restriction by major histocompatibility complex class I molecules or cell-to-cell contact. Instead, the activity is believed to be mediated by a heat-stable, acid-stable protein (*9*) with a molecular mass of <20 kD (*10*) or <10 kD (*11*). It is noteworthy that CAF inhibits HIV-1 replication irrespective of viral phenotype or tropism (*9*), but its precise mechanism of action remains unknown, although there are indications that the effect may be at the level of viral transcription (*12*, *13*).

Stimulated CD8 T lymphocytes release CAF in greater than normal abundance from HIV-1–infected persons who are doing well clinically, particularly those characterized as long-term nonprogressors (LTNPs) (*9*, *14*–*16*). In contrast, it is uncommonly detected in CD8 T cells from infected patients with evidence of immunodeficiency (progressors). CAF-like activity has been detected in stimulated CD8 T cells from SIV-infected rhesus macaques (*17*) or African Green monkeys (*18*), HIV-1–infected chimpanzees (*19*), and some healthy uninfected humans (*20*).

Despite tremendous efforts over the past 16 years (*9*), the identity of CAF has remained elusive. In 1995, Cocchi *et al.* (*21*) showed that stimulated CD8 T lymphocytes can secrete β-chemokines (RANTES and the macrophage inflammatory proteins MIP-1α and MIP-1β) that block HIV-1 infection in vitro. However, their antiviral activity was observed against macrophage-tropic viral isolates, but not against T cell line–tropic strains. This dichotomy was later explained by the discovery that the receptor for β-chemokines, CCR5, also serves as the coreceptor for HIV-1 entry into CD4 T cells (*22*–*24*). Thus, it became apparent that β-chemokines can competitively block so-called R5 viruses that use CCR5 as coreceptor, but not so-called X4 viruses that use an alternate coreceptor, CXCR4 (*25*). Such an antiviral profile clearly distinguished β-chemokines from CAF, which can inhibit both types of HIV-1. Moreover, CAF activity could not be eliminated by removing either β-chemokines (*26*, *27*) or SDF 1α (*28*), the ligand for CXCR4, with specific mAbs. Other cytokines have subsequently emerged as possible candidates for CAF, including macrophage-derived chemokine (*29*)

[1]Aaron Diamond AIDS Research Center, The Rockefeller University, 455 First Avenue, New York, NY 10016, USA. [2]Ciphergen Biosystems, Inc., 6611 Dumbarton Circle, Fremont, CA 94555, USA.

*To whom correspondence should be addressed. E-mail: lzhang@adarc.org (L.Z.); dho@adarc.org (D.D.H.)